Adv. Studies Theor. Phys., Vol. 4, 2010, no. 11, 511 - 524

Transmission Electron Features Revised: Quantum Field Theoretical Considerations

E. D. Cabanillas

CONICET and CNEA, Buenos Aires, Argentina

D. J. Cirilo-Lombardo

Bogoliubov Laboratory of Theoretical Physics, Dubna, Russian Federation.
and Departamento de Fisica, Universidade Federal da Paraiba, Joao Pessoa, PB Brazil
diego77jcl@yahoo.com

Abstract

In this work we discuss several aspects of the behaviour of the electrons in the interaction with the material scattered. The interpretation of the physical phenomena is helped through the TEM observation of diffraction microphotographs. From the pure quantum mechanical point of view we use the well known Born approximation to obtain the wave amplitude in a simple form in order to understand the problem roughly: electronic and probe features before the interaction, at the moment and after the interaction. Introducing the quantum field theoretical approach, the construction of new theoretical models that have account on the electron-phonon interaction in cristalline and amorphous samples is explicitly made. The comparison with the pure quantum mechanical results obtained previously and other models in the literature is briefly discussed.

1 Introduction and motivation: quantum mechanical considerations

The De Broglie postulate states that a particle having linear momentum has associated a wavelength . The experiments of G. P. Thompson and A. Reid, [1] and Davisson and Germer, [2] (published in the same Nature volume) gave the first evidence of the validity of the De Broglie postulate.

In transmission electron microscopy (TEM) observations, closely connected with the work of G. P. Thompson [1], electrons collide with and then go through matter. Afterwards they hit a screen, revealing the microscopic

details of the sample. We have observed by (TEM) a carbon steel sheet with a previous cold rolled mechanical treatment which induced a permanent magnetic field by plastic deformation. The sample to be examined by TEM was obtained by cutting a circular slice from the steel with an electro-spark erosion machine. The slice was electro-polished in a commercial "Struers" double jet device with a solution of 90% vol.acetic acid and perchloric acid 10% vol. at 15 °C and 30 V, to obtain a very thin zone. A TEM at an accelerating potential of 160 kV was used to obtain the pattern shown in Fig. 1 and the microscope was aligned in such a way that the electron beam, before introducing any sample, reached the centre of the screen.

The pattern of Fig. 1 shows a standard diffraction image of a steel sample but with all the spots shifted from the centre of the TEM screen.

Three different electron diffraction patterns can be observed by TEM showing the crystallinity of matter: a) amorphous, cf. Fig. 2; b) compound by a large number of very small crystallites, see Fig. 3; and c) formed by large single crystals cf. Figs. 1 and 4, [6]. If non ferromagnetic materials are observed, the central beam reaches the central part of the screen, see Fig. 4, but when a magnetized ferromagnetic sample is observed by TEM, the central beam is shifted from the centre of the screen, see Fig. 1.

Electrons are affected by magnetic induction and by electric fields. As inside of metals the electron field is null, the travelling electrons can interfere only with magnetic forces via the Lorentz formula:

$$\overrightarrow{F} = q\overrightarrow{v} \times \overrightarrow{B} \tag{1}$$

During its travel at velocity v through the magnetic sample, the particles (electrons) do not lose their charge and the internal induced magnetic field produces the necessary force to bend the electron beam inside the sample, eq. (1) . If the electron charge had disappeared, the central spot would not have moved from the central position. So, there is no doubt at all about the complementarity of the charge of the electron while it is behaving as a matter wave inside matter. If, for example, the sample were substituted by a non-magnetized one without changing any of the microscope conditions, the centred spot would appear in the centre of the screen.

In order to explain the electron diffraction pattern of Fig. 3 it is necessary to take into account some basic concepts from the former period of modern physics, i.e. the De Broglie wave length λ and the Bragg law, as it was done by G. P. Thompson, [1]. And in order to explain the electron pattern shown in Figs. 4 and 5, we have also to consider the Coulombian interaction between electrons and matter as a scattering problem, taking into account that matter is a tridimensional geometrical arrangement of ordered atoms. The micro world interactions are studied by means of quantum mechanics. The matter wave function $\Psi(r)$ associated with the electron satisfies the stationary

Schrödinger equation at all points of its trajectory. Electrons in a scattering experience have three different places where they are affected by the potential energy: a) before the sample, where the potential energy $V(r)$ is null, b) inside the sample, where the potential energy is deemed Coulombian and c) outside the sample where again the electron is not restricted to any potential but where $\Psi(r)$ has been strongly modified by the crystal interaction with matter and carries the useful information about the matter which has interacted.

In the first region, where $V(r) = 0$, the stationary Schrödinger equation is written as follows:

$$\nabla^2\Psi + k^2\Psi(r) = 0 \tag{2}$$

where E is the electron kinetic energy and the substitution $k^2 = \frac{\hbar^2}{2m}E$ has been used and whose well known solution is the plane wave function: $\Psi(r) = e^{ikr}$

In the second region, where the potential energy is given by the sample, it is difficult to find a wave function which could satisfy the Schrödinger equation. In order to write the wave function $\Psi(r)$ we can consider two types of approximations connected with two types of processes: elastic and inelastic. In the elastic process, the energy and the linear momentum are considered unaltered and in the inelastic one, the energy is altered by either excitation or ionization.

What is wanted is to obtain the electron wave function after its scattering with matter far from where the interaction takes place considering the elastic approximation process. The potential energy is restricted to the collision surroundings and the wave function amplitude tends to zero when the distance between sample and screen is large, that is why the intensity of the visual light that the impinging electrons produce on the fluorescent screen of the TEM diminishes. So the product $\Psi(r)V(r)$ tends to zero and the situation is called of "short range". The solution of the Schrödinger equation far away from the zone of interaction has to be proportional to e^{ikr} because $V(r) = 0$ and must have an asymptotic behaviour tending to zero.

The interaction region inside the sample, $V(r) = 0$, could be considered as a sphere of radius R. Far from the interaction region where $r >> R$, the potential energy could be considered as central and the solution of the Schrödinger equation could be obtained by the usual method of variable separation in spherical coordinates:

$$\Psi(r, \theta, \varphi) = R(r)\, Y_m^l(\theta, \varphi) \tag{3}$$

being $R(r)$ the radial function and $Y_m^l(\theta, \varphi)$ the spherical harmonics functions.

Considering the Hamiltonian correspondent to the radial part and the auxiliary function $u(r) = R(r)\, r$ the radial Schrödinger equation is written as

follows:

$$\left[-\frac{\hbar^2}{2m}\frac{d^2}{dr^2}+\frac{\hbar^2 l(l+1)}{2mr^2}+V\left(r\right)\right]u=Eu \tag{4}$$

But if the product $V(r)u(r)$ tends to zero and if $r >> R$, as it is in this case, the radial function that satisfies eq. with k given by eq.(3), is $u = e^{ikr}$ which is similar to the behaviour of the matter wave when $V(r)$ tends to zero and are called "short range potentials" [7].

Considering a short range potential, the matter wave must be free but if the impact parameter is larger than R, the particles will have different orbital momentum and the matter wave will consist of a superposition of all the orbital momentum states and it will be impossible to write the angular dependence with spherical harmonics, as it is used for radial potentials. Then, the solution of the Schrödinger equation will be $R(r) = u(r)/r$ times a function $f\left(\theta,\varphi\right)$, instead of the spherical harmonics $Y_m^l\left(\theta,\varphi\right)$, that is:

$$\Psi_{disp}\left(r,\theta,\varphi\right)=f\left(\theta,\varphi\right)u(r)/r \tag{5}$$

Screens or detectors are the devices which receive the scattered electrons, but both are far away from the target, and they receive scattered as well as non scattered electrons (whose function is $\Psi_{inc} = e^{ikz}$), so the dispersed wave function is expressed as the sum of both, the scattered and the non scattered:

$$\Psi_{disp}\left(r,\theta,\varphi\right)=e^{ikz}+f\left(\theta,\varphi\right)u(r)/r \tag{6}$$

where the incoming wave function e^{ikz} is expressed as a plane wave with its energy being the average energy of the ensemble system.

The parameter k in eq. and (10) is the modulus of the wave vector $\overrightarrow{k}$ which has the direction of the scattered wave and is also the modulus of the incident propagation vector $\overrightarrow{k}_0$ because of the energy conservation in the elastic consideration. $\overrightarrow{k}_0$ can be expressed as $\overrightarrow{k}_0 = k\overrightarrow{a}_z$, being $\overrightarrow{a}_z$ the unit vector of the direction of the incoming electrons. When the electrons hit the sample, an elastic interaction occurs and the only thing happening to the electron is the deviation of its trajectory, maintaining constant the modulus of the momentum, see Fig. 5. where it may be clearly seen how the electron changes its direction. Some extra momentum appears: $\overrightarrow{q} = 2\overrightarrow{k}Sin\left(\theta/2\right)$, then

$$\overrightarrow{k}=\overrightarrow{k}_0+\overrightarrow{q} \tag{7}$$

and another one has to come up on the sample, the backward momentum $-q$, which will not be considered here. The θ angle is the same angle seen in

electron diffraction and is the same which appears in the Bragg law: $2d\ Sin\theta = n\lambda$.

We now apply the Born approximation in order to solve the Schrödinger equation and compare its result with the previous method.

The Schrödinger equation in the interaction zone is

$$\left[-\frac{\hbar^2}{2m}\nabla^2 + V\right]\Psi = E\Psi \tag{7}$$

and from the relation $k^2 = \frac{\hbar^2}{2m}E$, the kinetic energy E can be rewritten as follows:

$$\left[\nabla^2 + k^2\right]\Psi = \frac{2m}{\hbar^2}V\Psi \tag{8}$$

We now compare the differential equation with the well-known differential equation in mathematical-physics:$\left[\nabla^2 + k^2\right]\Psi = -4\pi\rho$ whose solution is:

$$\Psi(r) = \int G(r, r')\, r' d^3\overrightarrow{r}' \tag{9}$$

where G is the Green function of and

$$\rho(r) = -\frac{mV(r)}{2\pi\hbar^2}\Psi(r) \tag{10}$$

is the inhomogeneity.

There are two Green functions for the operator $\nabla^2 + k^2$that appears in eq. (8) and (9) , $G_+ = e^{ikr}$ and $G_- = e^{-ikr}$ to assure the asymptotic behaviour of the function and the movement of the wave matter when $r > 0$ the G_+ is selected. Considering that r is the observation position and $r'$is the integration variable with $R = |r - r'|$ the Green function is wrtten as: $G_+ = e^{ik|r-r'|}$

So eq.(9) becomes:

$$\Psi(r) = -\frac{m}{2\pi\hbar^2}\int \frac{e^{ik|r-r'|}}{|r-r'|}V\left(\overrightarrow{r}\right)\Psi\left(\overrightarrow{r}\right)d^3\overrightarrow{r}' \tag{11}$$

The solution of the differential equation is the integral equation (11), so in order to obtain the general solution we have to consider the solution e^{ikz} of the homogeneous equation and the general solution is:

$$\Psi_{disp}(r, \theta, \varphi) = e^{ikz} - \frac{m}{2\pi\hbar^2}\int \frac{e^{ik|r-r'|}}{|r-r'|}V\left(\overrightarrow{r}\right)\Psi\left(\overrightarrow{r}\right)d^3\overrightarrow{r}' \tag{12}$$

As it was previously mentioned $V(r')$ is different from zero, in a very small spherical region of radius R as compared with r. With this assumption

we can think that the integration variable r'compared to r in $1/\left|r-r'\right|$ tends to $1/r$, and in the exponential the value $|r-r'|$tends to $|r-r'|\cdot r/r$ as the result of being developed in powers of r' tending to zero so the asymptotic solution becomes:

$$\Psi_{disp}\left(r,\theta,\varphi\right)=e^{ikz}-\frac{m}{2\pi\hbar^2}\frac{e^{ikr}}{r}\int e^{-ikr'}V\left(\overrightarrow{r}\right)\Psi\left(\overrightarrow{r}\right)d^3\overrightarrow{r}' \tag{13}$$

Iteration is the central point of the Born approximation and for the zero approximation term we may adopt:

$$\Psi_0\approx e^{ikz}=e^{i\overrightarrow{k}_0\overrightarrow{r}'} \tag{14}$$

And the first approximation solution is:

$$\Psi_{disp}\left(r,\theta,\varphi\right)=e^{ikz}-\frac{m}{2\pi\hbar^2}\frac{e^{ikr}}{r}\int e^{-ikr'}V\left(\overrightarrow{r}\right)e^{i\overrightarrow{k}_0\overrightarrow{r}'}d^3\overrightarrow{r}' \tag{15}$$

and with eq. (7), the last equation in (15) gives:

$$\Psi_{disp}\left(r,\theta,\varphi\right)=e^{ikz}-\frac{m}{2\pi\hbar^2}\frac{e^{ikr}}{r}\int e^{-i\overrightarrow{q}\cdot\overrightarrow{r}'}V\left(\overrightarrow{r}\right)d^3\overrightarrow{r}' \tag{16}$$

Comparing the last equations with (6):

$$\Psi_{disp}\left(r,\theta,\varphi\right)=e^{ikz}+f\left(\theta,\varphi\right)\frac{e^{ikr}}{r} \tag{17}$$

we can see that:

$$f\left(\theta,\varphi\right)=-\frac{m}{2\pi\hbar^2}\frac{e^{ikr}}{r}\int e^{-i\overrightarrow{q}\cdot\overrightarrow{r}'}V\left(\overrightarrow{r}\right)d^3\overrightarrow{r}' \tag{18}$$

is the Fourier transformation of the potential energy $V(r)$.

The importance of the calculation of $f\left(\theta,\varphi\right)$ in scattering theory is connected to the cross section; in solid physics it is the amplitude of the dispersed wave function used to obtain the same Laués relation and of course the Braggś law as is done with x-rays instead of electrons and the superposition in a diffraction effect of wave functions, [5].

2 Second quantization approach: the structure of the lattice

The electron will polarize its surrounding and in its motion will carry the polarization cloud around it. The electron and the cloud constitute a quasiparticle. The polarization of the surroundings means a distortion of the lattice,

hence an excitation of optical phonons. The quasi-particle can be described as an electron surrounded by a cloud of (virtual) optical phonons. It is called a "polaron". One of its most important properties is an increased inert mass.

The model describing a polaron will depend on whether the distortion of the lattice is limited to the immediate vicinity of the electron (small polaron) or whether it extends over several lattice constants (large polaron). The large polaron case is the most representative for scattering experiments. In order to perform the computations in the second quantization approach we can use the continuum approximation [8].

Firstly we are expressing the coefficients b_{ik} of the Wigner-Seitz lattice in terms of $\varepsilon(0)$, $\varepsilon(\infty)$ and the limiting frequency of the longitudinal optical branch ω_L, then

$$\overline{P} = -\varepsilon_0 \overline{E} = \frac{\varepsilon_0 b_{21}}{\varepsilon_0 + b_{22}} \overline{w} = \left\{ \frac{N\overline{M}\omega_L \varepsilon_0}{V_g} \left[\frac{1}{\varepsilon(0)} - \frac{1}{\varepsilon(\infty)} \right] \right\}^{1/2} \overline{s} \tag{19}$$

The interaction energy of an electron with the polarized medium is

$$H_{el-ph} = -\frac{e}{4\pi\varepsilon_0} \int \frac{\overline{P}(\overline{r})(\overline{r} - \overline{r}_{el})}{|\overline{r} - \overline{r}_{el}|^3} dr \tag{20}$$

Inserting (19) in (20) and using the quantized form in the continuum approximation of $\overline{s}(\overline{r}, t)$ we can easily solve the problem: we must connect $\overline{s}(\overline{r}, t)$ with the discrete displacements in the lattice $\overline{s}_{n\alpha}$.Taking a binary lattice, longitudinal vibrations obey

$$e_\alpha(\overline{q}) = e_\alpha^*(-\overline{q}) \qquad \text{are } // \text{ to } \overline{q} \tag{21}$$

this fact give us (see [8])

$$\overline{s}_n \frac{1}{\sqrt{N\overline{M}}} \sum_{\overline{q}} Q_{\overline{q}} \frac{\overline{q}}{q} exp(i\overline{q} \cdot \overline{R}_n) \tag{22}$$

with

$$Q_{\overline{q}} = \left(\frac{\hbar}{2\omega_L} \right)^{1/2} \left(a_{-\overline{q}}^+ + a_{\overline{q}} \right) \quad ; \quad \overline{M} : \text{reduced mass of the binary lattice} \tag{23}$$

Here the summation over j is omitted since we are only considering the LO branch and the limiting value ω_L for the the optical vibration frequency. The dependence of the LO branch can be neglected where the continuum approximation is valid. Finally:

$$\overline{s}(\overline{r}) = \left(\frac{\hbar}{2N\overline{M}\omega_L} \right)^{1/2} \sum_{\overline{q}} \frac{\overline{q}}{q} \left[a_{\overline{q}}^+ exp(-i\overline{q} \cdot \overline{r}) + a_{\overline{q}} exp(i\overline{q} \cdot \overline{r}) \right] \tag{24}$$

only the 2 exponential factors are now $\overline{r}$-dependents and the integral in the H_{el-ph} is easy to carry out. Since

$$\int \frac{exp(\pm i\overline{q}\cdot\overline{r})\,(\overline{r}-\overline{r}_{el})}{|\overline{r}-\overline{r}_{el}|^3}d\tau = \mp 4\pi i\frac{\overline{q}}{q^2}exp(\pm i\overline{q}\cdot\overline{r}_{el}) \tag{25}$$

then

$$H_{el-ph} = i\left\{\frac{e^2\hbar\omega_L}{2\varepsilon_0 V_g}\left[\frac{1}{\varepsilon\,(0)}-\frac{1}{\varepsilon\,(\infty)}\right]\right\}^{1/2}\sum_{\overline{q}}\frac{1}{q}\left[-a^{+}_{\overline{q}}exp(-i\overline{q}\cdot\overline{r}_{el})+a_{\overline{q}}exp(i\overline{q}\cdot\overline{r}_{el})\right] \tag{26}$$

From the perturbative QFT we know that the zero order wave functions are the plane waves extended by the vacuum state $|0;0\rangle$of the phonon system, being the zero order energy $E^{(0)}_{(\overline{k})}=\frac{\hbar^2k^2}{2m}$. The states over which the additional terms are summed are states where an optical phonon of energy$\overline{q}$ and wave number $\hbar\omega_L$is emitted. Then

$$\left|\overline{k};0\right\rangle^{(1)} = \left|\overline{k};0\right\rangle^{(0)} + \sum_{\overline{q}}\frac{\left\langle\overline{k}-\overline{q};1_{\overline{q}}\left|H_{el-ph}\right|\overline{k};0_{\overline{q}}\right\rangle}{E^{(0)}_{(\overline{k})}-E^{(0)}_{(\overline{k}-\overline{q})}-\hbar\omega_L}\left|\overline{k}-\overline{q};1_{\overline{q}}\right\rangle^{(0)} \tag{27}$$

$$E^{(1)}_{(\overline{k})} = E^{(0)}_{(\overline{k})} + \sum_{\overline{q}}\frac{\left|\left\langle\overline{k}-\overline{q};1_{\overline{q}}\left|H_{el-ph}\right|\overline{k};0_{\overline{q}}\right\rangle\right|^2}{E^{(0)}_{(\overline{k})}-E^{(0)}_{(\overline{k}-\overline{q})}-\hbar\omega_L} \tag{28}$$

that can easily be computed having account of the matrix element

$$\left\langle\overline{k}-\overline{q};1_{\overline{q}}\left|H_{el-ph}\right|\overline{k};0_{\overline{q}}\right\rangle = -\frac{i}{q}\left\{\frac{e^2\omega_L}{2\varepsilon_0 V_g}\left[\frac{1}{\varepsilon\,(0)}-\frac{1}{\varepsilon\,(\infty)}\right]\right\}^{1/2} \tag{29}$$

Now, considering the pure quantum mechanical expression (16) and expression (27), the relation between the potential $V\,(\overline{r}')$ and the specific structure of the lattice in the sample is easily obtained:

$$-i\sum_{\overline{q}}\frac{1}{\left(\frac{\hbar^2q^2}{2m}-\hbar\omega_L\right)}\left\{\frac{e^2\hbar\omega_L}{2\varepsilon_0 V_g}\left[\frac{1}{\varepsilon\,(0)}-\frac{1}{\varepsilon\,(\infty)}\right]\right\}^{1/2} = -\frac{m}{2\pi\hbar^2}\int V\,(\overline{r}')\,exp(-i\overline{q}\cdot\overline{r})d^3r' \tag{30}$$

3 Scattering in amorphous solid bodies: the new quantized model

Our starting point is the Hamiltonian electron-phonon (20) but now $\overline{P}$ is the corresponding to the *amorphous isotropic* case. There are in such case two characteristic velocities of sound propagation: u_l and u_t (longitudinal and transversal respectively). As is more or less known, the main consequences of these two velocities u_l and u_t are that the Rayleigh line contains two Mandelstam-Brillouin's doublets and they are closely related with the scattering by longitudinal and transversal acoustic waves, being from the center of the line $\pm \triangle \omega_l$ and $\pm \triangle \omega_t$ where: $\triangle\omega_l = qu_l$; $\triangle\omega_t = qu_t$.

Now, as in [9]

$$P^h = \frac{-\omega^2 e^{ikr}}{4\pi r c^2} \epsilon_{ig}{}^h \epsilon^{ijk} n'_h n'_j G_k \tag{31}$$

where

$$G_i = \int \delta G_{ik} e^{-iqr} F_0{}^k dV \qquad (F_{k0} \equiv E_k) \tag{32}$$

$F_{k0} \equiv E_k$ is the incident field and $\overline{n}'$ is the unitary scattering vector. The variation of the permittivity by the deformation of an isotropic amorphous body is[9]

$$\delta G_{ik} = a_1 u_{ik} + a_2 u_{ll} \delta_{ik} \tag{33}$$

where u_{ik} is the tensor of deformations, obviously, that can be written as a function of the displacement vector: $u_i = \frac{1}{2}\left[u_{0i} e^{iqr} + u^*_{0i} e^{-iqr}\right]$. Then

$$u_{ik} = \frac{i}{4}\left[\left(u_{0i} q_k + u_{0k} q_i\right) e^{iqr} + \left(u^*_{0i} q_k + u^*_{0k} q_i\right) e^{-iqr}\right] \tag{34}$$

and the volume integral takes the following simple form

$$\int \left(u_{ik} e^{-iqr} + u^*_{ik} e^{iqr}\right) dV = \frac{iV}{4}\left[\left(u_{0i} q_k + u_{0k} q_i\right) + \left(u^*_{0i} q_k + u^*_{0k} q_i\right)\right] \tag{35}$$

As in the crystal case that was treated before, all the fields can be expressed as functions of the displacements then, the Hamiltonian remains with the same form as in (20) but now with P given by (31):

$$H_{el-ph} = -\frac{e}{4\pi\varepsilon_0} \int \frac{-\omega^2 e^{ikr}}{4\pi r c^2} \epsilon_{ig}{}^h \epsilon^{ijk} n'_h n'_j G_k \omega_h dr \; ; \qquad with: \; \omega_h \equiv \frac{(\overline{r} - \overline{r}_{el})}{|r - r_{el}|^3} \tag{36}$$

To obtain the explicit form of G_i we use the expressions (33)-(35) in (32), then

$$G_i = \frac{i}{4} V \left[a_1 \left(u_{0i} q_k + q_i u_{0k} \right) F^{\ 0k} + 2 a_2 F^0_{\ i} u_0^{\ k} q_k \right] \tag{37}$$

As is easily seen, in order to pass to the quantized version, the displacements must to be written as functions of the standard annihilation and creation operators $\widehat{a}$ and $\widehat{a}^+ \rightarrow \widehat{u}_{0i} = \frac{u_{0i}}{\sqrt{2}} \left(\widehat{a} + \widehat{a}^+ \right)$.Then

$$\left\langle \overline{k} - \overline{q}; 1_{\overline{q}} \left| H_{el-ph} \right| \overline{k}; 0_{\overline{q}} \right\rangle$$

$$= -\frac{e^{i\overline{k} \cdot \overline{r}_{el}}}{\overline{r}^2_{el}} \left(i\overline{k} \cdot \overline{r}_{el} - 1 \right) \left(\frac{i}{4k^2} \frac{e}{\left(4\pi \right)^2 \varepsilon_0} \frac{\omega^2}{c^2} \right) V \left[a_1 \left(u_{0i} q_k + q_i u_{0k} \right) F^{\ 0k} + 2 a_2 F^0_{\ i} u_0^{\ k} q_k \right]$$

The advantage of this formulation from others [10] is clear: expressions (36) -(38) have the correct limit coming from the quantized model to the classical case.

4 Concluding remarks:

In this work several aspects of the behaviour of the electrons in the interaction with the material scattered have been described and new models were presented

From the quantum theoretical point of view, and helped through the TEM observation of diffraction microphotographs, the basis of this interesting physical phenomenon was carefully explained.

The well known Born approximation was used obtaining the wave amplitude in a simple form in order to understand roughly the problem: electronic and probe features before the interaction, at the moment and after it.

From the quantum field theoretical approach, the construction of new theoretical models that have account on the electron-phonon interaction in crystalline and amorphous samples was explicitly made.

With the QFT approach the relation between the potential $V\left(\overline{r}'\right)$ included into the Born approximation and the specific structure of the sample was easily obtained, then the meaning of $f\left(\theta, \varphi\right)$ in the scattering of solids was elucidated.

Finally, it is interesting to note that similar models describing scattering in amorphous samples as in [10], although fit with some degree quantum aspects of the phenomena, do not have the correct classical limit.

Acknowledgements

EDC acknowledge the financial support given by CNEA-CONICET, and one of us DJCL is very grateful to the Atomic Center Constituyentes (CNEA-CAC) where this work begin and to the Bogoliubov Laboratory of Theoretical Physics JINR-Dubna-Russian Federation and to the Department of Physics of the University Federal de Paraiba for their hospitality and the RFBR-Russia and CAPES-Brazil for financial support.

References

[1] G. P. Thompson and A. Reid, "Diffraction of Cathode Rays by a Thin Film" Nature 119, 890-890 (1927).

[2] C. Davisson and L. H. Germer, The scattering of electrons by a single crystal of nickel, Nature 119 558-560 (1927).

[3] C. Kittel, Introduction to Solid State Physics (John Wiley and Sons Inc., New York, 5 th edition).

[4] N. W. Ashcroft and N. D. Mermin, Solid State Physics (Saunder College Publishing, New York, 1976).

[5] A. Howie, P. B. Hirsch, R. B. Nicholson, D. W. Pashly and M. J. Whelan, Electron microscopy of thin crystals (Butterworths, 1965).

[6] L. E. Murr, Electron Optical Applications in Materials Science, (Mc. Graw-Hill Series in Materials Science and Engineering, Mc. Graw-Hill Book Company New York 1970).

[7] Luis de la Peña, Introducción a la Mecánica Cuántica, (Chap. 13, CECSA Compañía Editorial Continental S. A., México. First Edition 1979).

[8] O. Madelung, "Introduction to solid state physics" (Springer Series in solid state sciences, Berlin, 1978).

[9] L. Landau and E. Lifshitz, "Electrodinamica de los Medios Continuos" (Editorial Reverte, Buenos Aires, 1981).

[10] see for example Mingliang Zhang et al. http://arxiv.org/abs/0805.2575v2

Figures

Figure 1: Electron diffraction pattern of a magnetized steel, see the central spot not coincident with the centre of the micrograph

Figure 2: Electron diffraction pattern of an amorphous sample, see the circular rings

Figures

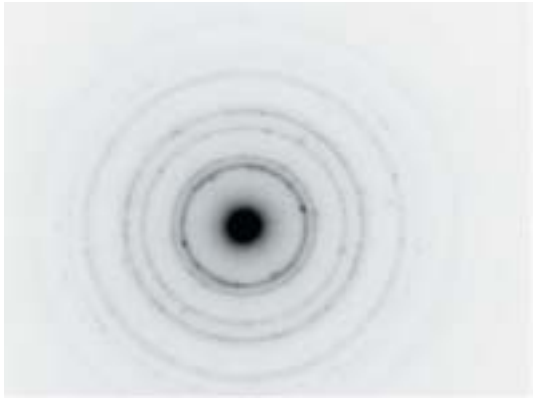

Figure 3: Electron diffraction pattern of an amorphous sample, see the circular rings

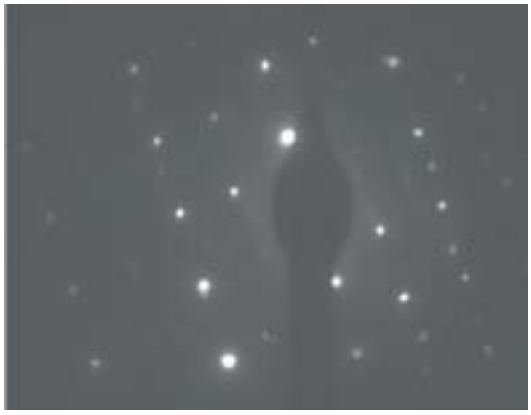

Figure 4: Electron diffraction pattern obtained from a large single crystal

Figures

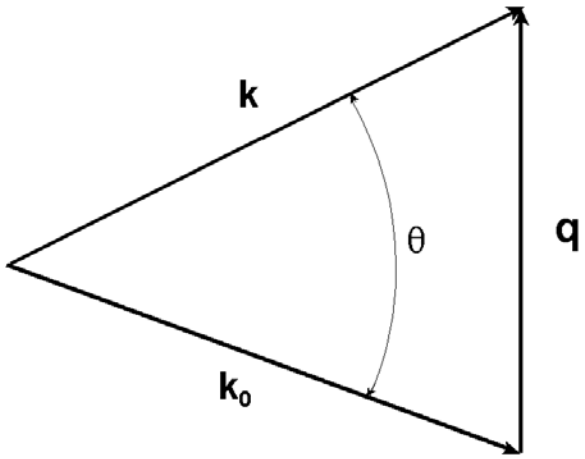

Figure 5: Diagram of linear momentum interchange

Received: February, 2010